Digestive and Liver Disease 51 (2019) 985–992

Contents lists available at ScienceDirect

Digestive and Liver Disease

journal homepage: www.elsevier.com/locate/dld

Digestive Endoscopy

Noninvasive prediction model for diagnosing gastrointestinal stromal tumors using contrast-enhanced harmonic endoscopic ultrasound

In Rae Cho[a], Jun Chul Park[b,c,*], Yun Ho Roh[d], Soo In Choi[b], Jeung Eun Lee[b], Eun Hye Kim[b,c], Sung Kwan Shin[b,c], Sang Kil Lee[b,c], Yong Chan Lee[b,c]

[a] Department of Internal Medicine, Catholic Kwandong University College of Medicine, Incheon, Republic of Korea
[b] Department of Internal Medicine, Yonsei University College of Medicine, 03722, Seodaemun-gu, Seoul, Republic of Korea
[c] Institute of Gastroenterology, Yonsei University College of Medicine, Seoul, Republic of Korea
[d] Biostatistics Collaboration Unit, Yonsei University College of Medicine, Seoul, Republic of Korea

ARTICLE INFO

Article history:
Received 21 September 2018
Accepted 25 February 2019
Available online 27 March 2019

Keywords:
Contrast-enhanced harmonic endoscopic ultrasound
Gastrointestinal stromal tumor
Leiomyoma
Subepithelial tumor

ABSTRACT

Background & Aims: Subepithelial tumors (SETs) are difficult to diagnose accurately without invasive pathological confirmation. We created a noninvasive prediction model for diagnosing gastrointestinal stromal tumors (GISTs) using contrast-enhanced harmonic endoscopic ultrasound (CEH-EUS).
Methods: We retrospectively reviewed 176 patients who underwent CEH-EUS from October 2011 to August 2017. Seventy patients with a diagnosis of GIST (n = 37) or leiomyoma (n = 33) were included. The long-to-short axis ratio (LSR) and enhancement patterns (vascularity, diffuse enhancement) on CEH-EUS were assessed. Logistic regression and classification and regression tree (CART) analyses were performed.
Results: The mean age of all patients was 54.9 ± 13.68 years. The GIST group showed significantly higher rates of positive vascularity (81.1% vs. 15.2%, $p < 0.001$) and diffuse enhancement (51.4% vs. 15.2%, $p = 0.001$), and lower LSR (1.30 vs. 1.76, $p < 0.001$). In multivariate logistic regression, positive vascularity (odds ratio [OR] 27.765, 95% confidence interval [CI] 5.336–144.458) and low LSR (OR 18.940, 95% CI 3.623–99.007) were independent predictors of GIST. A noninvasive prediction model for GISTs was developed using the CART model, by allocating patients according to statistically significant variables.
Conclusions: The LSR and vascularity of SETs on CEH-EUS can be used as parameters for a noninvasive prediction model of GISTs. This model may be helpful in the early identification and treatment of GISTs.
© 2019 Editrice Gastroenterologica Italiana S.r.l. Published by Elsevier Ltd. All rights reserved.

1. Introduction

Subepithelial tumors (SETs) of the gastrointestinal tract have become a clinical challenge for gastroenterologists. Although SETs are usually detected incidentally and show a low prevalence, the recent increase in screening esophagogastroduodenoscopy procedures has led to the increase in the rates of SET diagnosis, causing a growing interest in the treatment strategy for these tumors [1,2]. Most SETs do not cause symptoms and show a benign course. However, some types of SETs, such as neuroendocrine tumors, lymphomas and gastrointestinal stromal tumors (GISTs) have a malignant potential. The location, layer of origin, and echotexture of a SET under endoscopic ultrasound (EUS) have been used for the differential diagnosis of these gastrointestinal tract tumors and may be diagnostic in some cases. Nevertheless, EUS imaging alone is insufficient to accurately diagnose hypoechoic SETs, especially those originating from the fourth (muscularis propria) layer, where diverse SETs can originate [3,4]. Among them, GISTs and leiomyomas are the most commonly identified intramural SETs in the upper gastrointestinal tract [5,6]. The differential diagnosis of these 2 tumor types is important because 10–30% of GISTs can be malignant whereas malignant transformation of leiomyomas is extremely rare [7].

Several methods have been used for tissue acquisition from SETs in the gastrointestinal tract. EUS-guided fine-needle aspiration (EUS-FNA) is the most widely used method. However, the diagnostic accuracy of EUS-FNA ranges widely from 46% to 93%, and the overall diagnostic yield of small lesions is only 40–50% [8,9]. Recently, EUS-guided fine-needle biopsy and the "unroofing" biopsy technique (mucosal incision-assisted biopsy) have been used for the histological evaluation of SETs [10,11] and have shown higher diagnostic yield compared with EUS-FNA [12,13]; however, the data remain insufficient and such procedures need to be per-

* Corresponding author at: Division of Gastroenterology, Department of Internal Medicine, Yonsei University College of Medicine, 50-1 Yonsei-ro, Seodaemun-gu, Seoul 03722, Republic of Korea.
E-mail address: junchul75@yuhs.ac (J.C. Park).

https://doi.org/10.1016/j.dld.2019.02.017
1590-8658/© 2019 Editrice Gastroenterologica Italiana S.r.l. Published by Elsevier Ltd. All rights reserved.

formed by an expert owing to technical difficulties and the risk of complications.

Therefore, in the clinical field, there is a need for a noninvasive and accurate diagnostic method for SETs. A noninvasive diagnostic model of SETs would benefit both patients and physicians because it can lead to early diagnosis and help avoid unnecessary invasive procedures for tissue acquisition. Contrast-enhanced harmonic EUS (CEH-EUS) is a relatively new ultrasonic imaging method for the differential diagnosis of SETs and pancreatic mass lesions. Although there have been attempts to differentiate SETs using CEH-EUS, some limitations remain in the diagnosis of GISTs using CEH-EUS findings alone [14,15]. Therefore, further investigations are needed to establish a noninvasive diagnostic prediction model including parameters of CEH-EUS and other clinical factors.

The aims of this study were to establish a noninvasive prediction model of GISTs, and to confirm the usefulness and accuracy of this prediction model.

2. Material and methods

2.1. Study patients

Patients who underwent CEH-EUS because of SETs in the upper gastrointestinal tract between October 2011 and August 2017 were retrospectively reviewed (n = 176). Among them, patients without pathological confirmation (n = 75) and those without adequate pathological results after EUS-guided fine-needle biopsy (n = 31; 18 mucosal tissue, 7 fibrous tissue, 3 ectopic pancreas, 1 fibromatosis, 1 gastric cystica profunda, and 1 anisakiasis) were excluded. Finally, 70 patients with a pathological diagnosis of GIST (GIST group, n = 37) or leiomyoma (leiomyoma group, n = 33) were included and analyzed (Fig. 1).

After the enrollment of eligible patients, the following parameters were investigated and recorded: patient demographics, location of SET, presence of mucosal erythema and ulceration, size of SET, and endosonographic features with contrast enhancement.

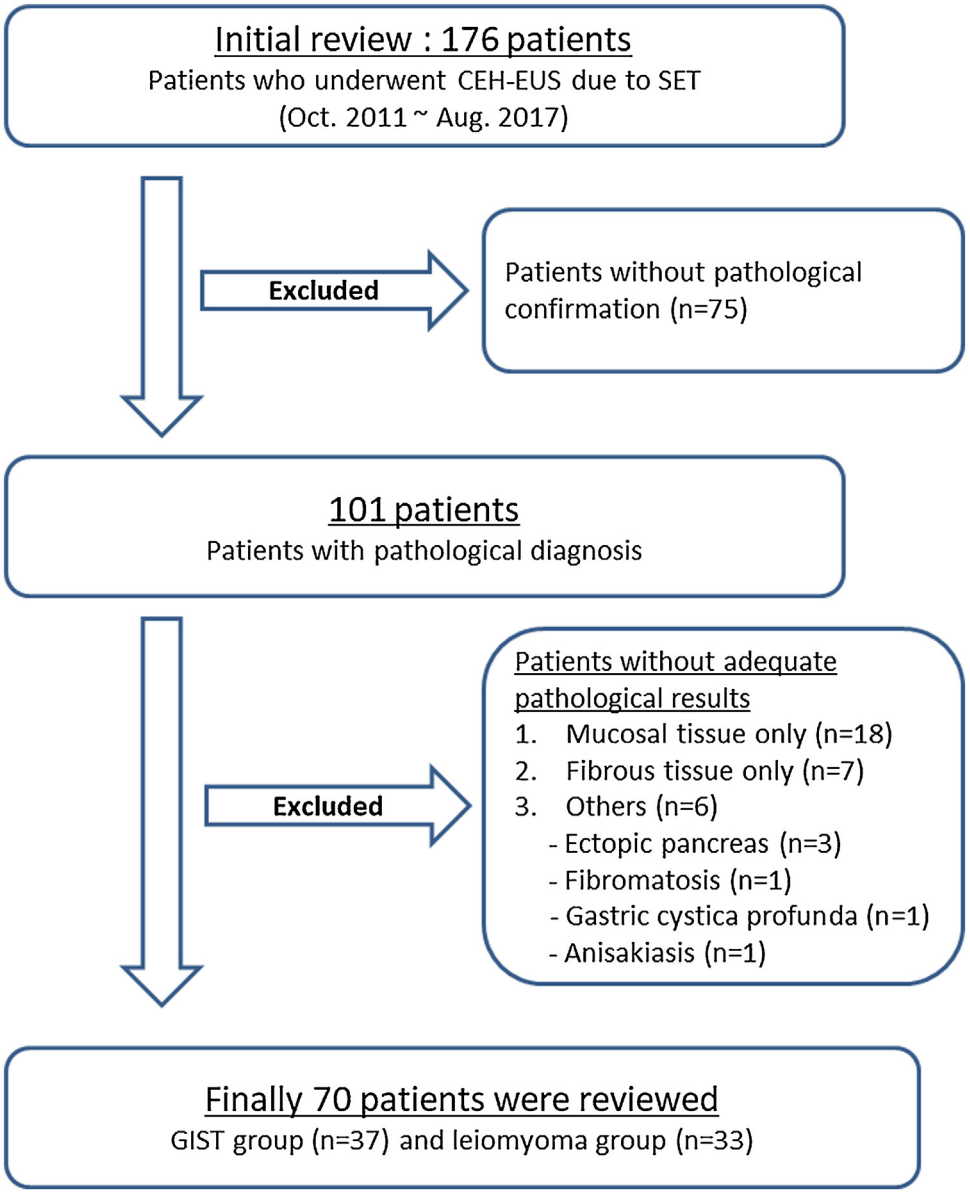

Fig. 1. Flow diagram showing the eligibility assessment, enrollment, group allocation, and analysis of study participants.

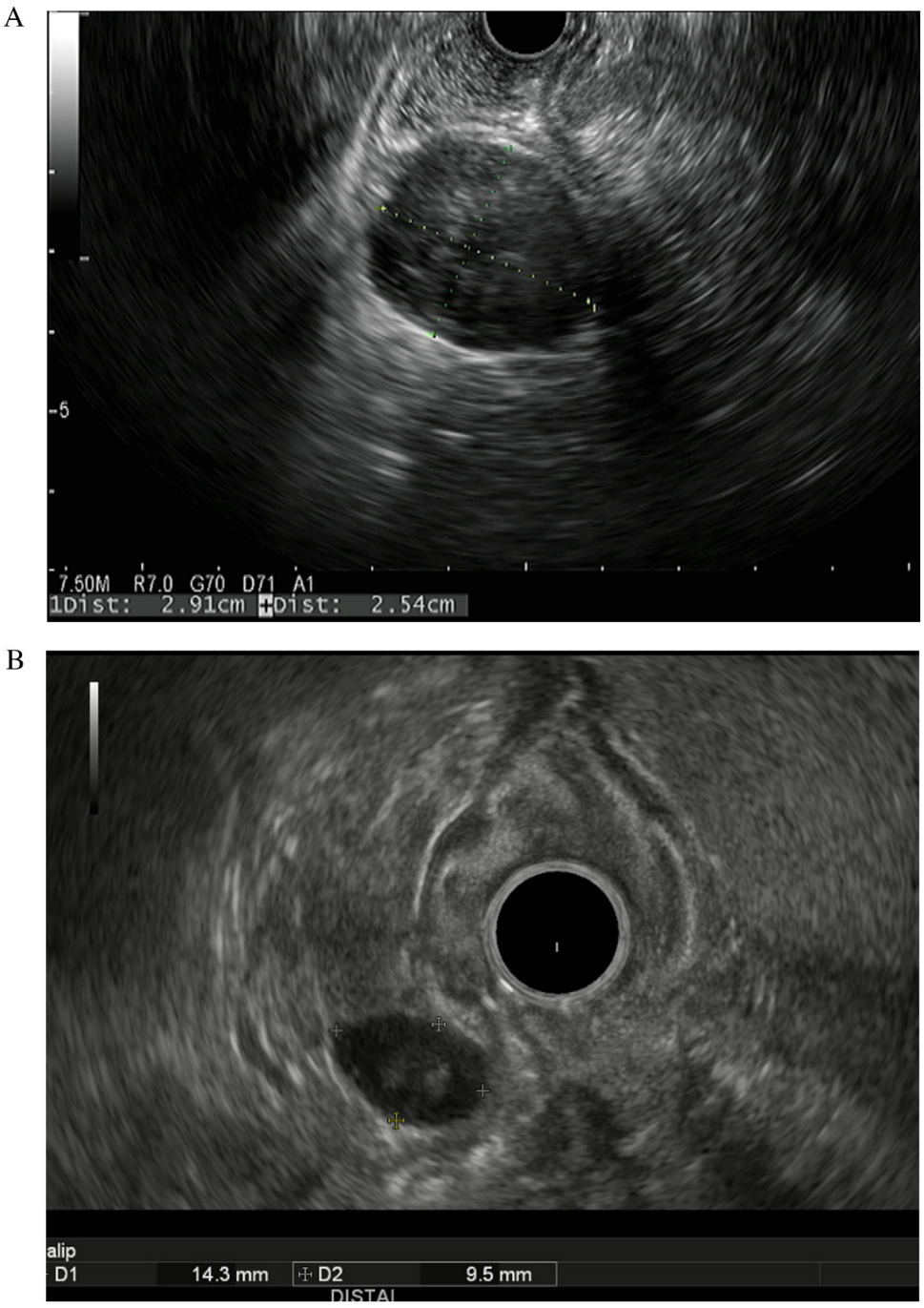

Fig. 2. The long-to-short ratio (LSR) was calculated under B-mode. (A) A round-shaped subepithelial tumor (SET) with a low LSR (=1.15) and (B) an oval-shaped SET with a high LSR (=1.51).

This study was approved by the Yonsei University Health System Institutional Review Board (1-2018-0020) and conducted in accordance with the principles set forth in the Declaration of Helsinki.

2.2. Endosonographic evaluation and parameters—B-mode and CEH-EUS

All patients underwent 2-dimensional B-mode EUS before CEH-EUS for the evaluation of SETs. The size and length of the long and short axis, layer of origin, echogenicity, homogeneity, and existence of echogenic spots were documented. EUS examinations were performed by an experienced endosonographer (JC Park) using an Olympus GF-UE260P echoendoscope (Olympus Medical Systems Co., Ltd., Tokyo, Japan) and ALOKA Prosound Alpha-10 processor (ALOKA Co., Ltd., Tokyo, Japan). For CEH-EUS, the extended pure harmonic detection mode was used, which combines the filtered fundamental and second harmonic component frequencies with a transmitting frequency of 4.7 MHz.

The long-to-short ratio (LSR), defined as the ratio between the length of the long and short axes of the SET, can be simply calculated under conventional B-mode (Fig. 2). The patients were divided into 2 groups (low LSR and high LSR) according to the LSR cut-off value of 1.475 (area under the receiver-operating characteristic curve [AUROC] 0.856).

After a bolus injection of contrast agent (2.5 mg SonoVue) and flushing with saline (10 mL), the enhancement pattern of SETs on

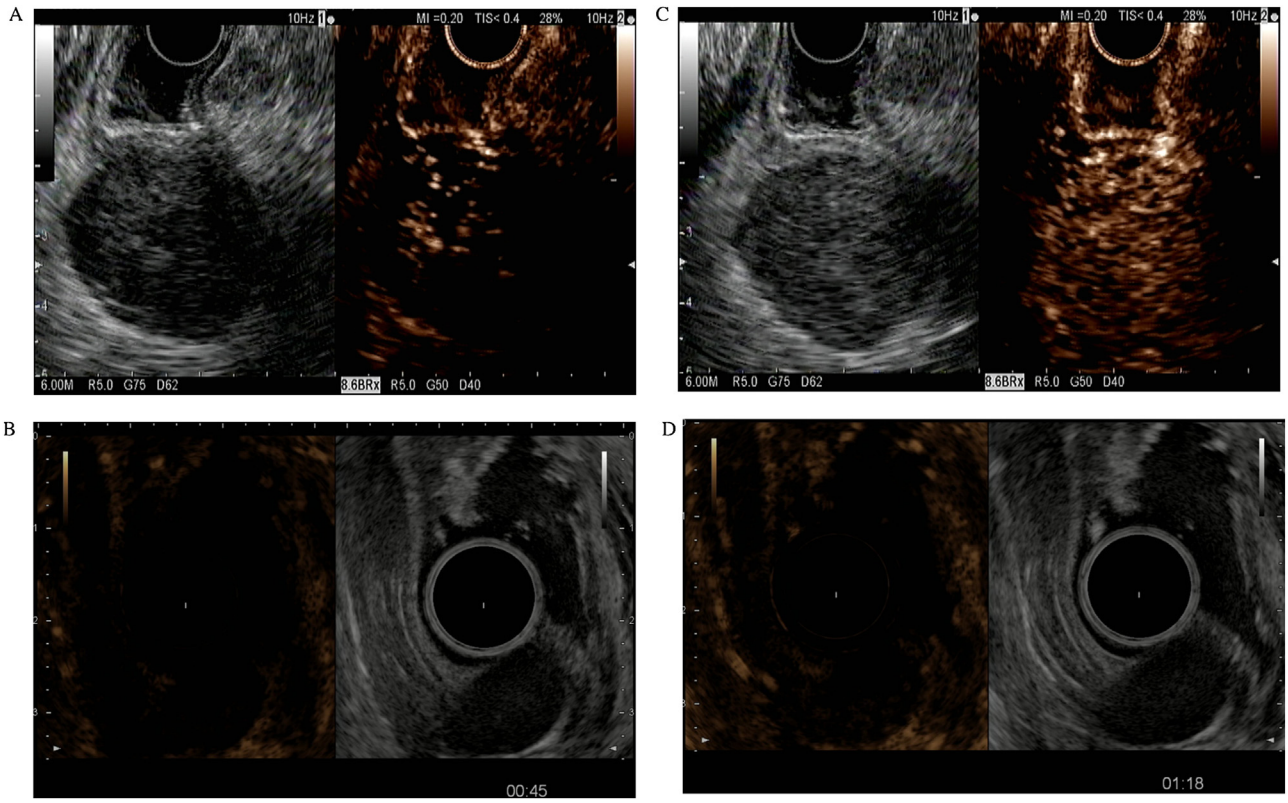

Fig. 3. After SonoVue administration, vascularity and diffuse enhancement were assessed. (A) Vascularity was seen inside the subepithelial tumor (SET) in the early phase. (B) Vascularity was not seen until 50 s after injection. (C) Diffuse enhancement in the venous phase was seen inside the SET. (D) Diffuse enhancement in the venous phase was not seen.

CEH-EUS was assessed in real time. Adopting the definition from the European Federation of Societies for Ultrasound in Medicine and Biology guidelines, 2 phases of enhancement patterns were investigated for the timing of enhancement: arterial phase, usually starting from 10 to 20 s (first arrival of contrast) to around 30 to 45 s, and venous phase, which starts from approximately 30 to 45 s after contrast injection [16,17]. The presence of linear enhancement in the arterial phase was defined as positive vascularity, whereas no enhancement or unorganized artifacts were considered as negative vascularity. Because linear enhancement was similar to the shape of the micro vessel inside the SET, it is thought to represent vessel flow in the early arterial phase. Additionally, iso- or hyper-enhancement inside the SET, relative to surrounding tissues, in the venous phase was defined as diffuse enhancement (Fig. 3).

2.3. Statistical analysis

Continuous variables are expressed as mean ± standard deviation if data were normally distributed, or as median (interquartile range) otherwise. Student's t-test or Mann Whitney U-test was used to compare continuous variables, and chi-square test or Fisher's exact test was used to compare categorical variables. Values with $p < 0.05$ were considered statistically significant. The receiver-operating characteristic curve with the maximum Youden index was analyzed to obtain the optimal cutoff value of LSR that discriminates GISTs and leiomyomas. Univariable and multivariable logistic regression models were used to estimate independent predictors of a GIST diagnosis. The sensitivity, specificity, positive predictive value (PPV), negative predictive value (NPV), and accuracy for GIST diagnosis were also calculated. We performed classification and regression tree (CART) analysis to develop models for predicting a GIST diagnosis. The CART analysis was conducted using R statistical package 'rpart' (available from the R Foundation, http://cran.r-project.org/web/packages/rpart/rpart.pdf). The other data were analyzed using IBM SPSS Statistics for Windows, version 23.0 (IBM Corp., Armonk, NY, USA).

3. Results

3.1. Baseline characteristics

The baseline characteristics of all patients are summarized in Table 1. The mean age of all patients was 54.9 years, and patients in the leiomyoma group were significantly younger than those in the GIST group (49.6 vs. 59.6 years, $p = 0.002$). The most common location of SETs was the gastric body ($n = 25$, 35.7%) followed by the gastric cardia/fundus ($n = 23$, 32.9%) and esophagus ($n = 15$, 21.4%). The mean size and LSR of SETs were 2.46 cm and 1.51, respectively. There was no significant difference in the size of SETs between the 2 groups (2.61 vs. 2.29 cm, $p = 0.342$). However, the LSR of the GIST group was significantly lower than that of the leiomyoma group (1.30 vs. 1.76, $p < 0.001$) (Supplemental Fig. 1). Of the patients, 50% ($n = 35$) showed positive vascularity and 34.3% showed diffuse enhancement in the venous phase. The rates of positive vascularity (81.1% vs. 15.2%, $p < 0.001$) and diffuse enhancement (51.4% vs. 15.2%, $p = 0.001$) were significantly higher in the GIST group.

3.2. Non-invasive predictors of GIST diagnosis

A logistic regression model was used to find the noninvasive predictors of a GIST diagnosis (Table 2). In univariate analysis, the LSR, vascularity, and diffuse enhancement showed statistical significance. In multivariate analysis, vascularity (odds ratio [OR] 27.765, 95% confidence interval [CI] 5.336–144.458) and the

Table 1
Baseline characteristics and endoscopic ultrasound findings of all patients.

Variables	All patients (n = 70)	GIST (n = 37)	Leiomyoma (n = 33)	p
Age, years	54.9 (±13.68)	59.6 (±13.68)	49.6 (±11.74)	0.002
Sex				0.300
Male	40 (57.1%)	19 (51.4%)	21 (63.6%)	
Female	30 (42.9%)	18 (48.6%)	12 (36.4%)	
Tumor location				<0.001
Esophagus	15 (21.4%)	0 (0%)	15 (45.5%)	
Cardia/fundus	23 (32.9%)	7 (18.9%)	16 (48.5%)	
Body	25 (35.7%)	24 (64.9%)	1 (3.0%)	
Antrum	5 (7.1%)	4 (10.8%)	1 (3.0%)	
Duodenum	2 (2.9%)	2 (5.4%)	0 (0%)	
Mucosal lesion				
Ulceration	4 (5.7%)	3 (8.1%)	1 (3.0%)	0.616
Erythema	10 (14.3%)	8 (21.6%)	2 (6.1%)	0.090
Lesion size, cm	2.46 (±1.38)	2.61 (±1.71)	2.29 (±0.88)	0.342
LSR	1.51 (±0.38)	1.30 (±0.20)	1.76 (±0.38)	<0.001
Vascularity				<0.001
No	35 (50.0%)	7 (18.9%)	28 (84.8%)	
Yes	35 (50.0%)	30 (81.1%)	5 (15.2%)	
Diffuse enhancement				0.001
No	46 (65.7%)	18 (48.6%)	28 (84.8%)	
Yes	24 (34.3%)	19 (51.4%)	5 (15.2%)	

GIST, gastrointestinal stromal tumor; LSR, long-to-short ratio.

Table 2
Logistic regression model for independent predictors of gastrointestinal stromal tumor.

	Univariate analysis		Multivariate analysis		Univariate analysis[a]		Multivariate analysis[a]	
	OR (95% CI)	p	OR (95% CI)	p	OR (95% CI)	p	OR (95% CI)	p
Vascularity (arterial phase)								
No	1		1		1		1	
Yes	24.000 (6.822–84.433)	<0.001	27.765 (5.336–144.458)	<0.001	11.143 (2.979–41.684)	<0.001	15.184 (2.809–82.062)	0.002
Diffuse enhancement (venous phase)								
No	1				1			
Yes	5.911 (1.873–18.657)	0.002			3.694 (1.022–13.350)	0.046		
LSR								
>1.475	1		1		1		1	
≤1.475	16.146 (4.950–52.669)	<0.001	18.940 (3.623–99.007)	0.001	10.133 (2.779–38.420)	<0.001	14.280 (2.593–78.637)	0.002

OR, odds ratio; CI, confidence interval; LSR, long-to-short ratio.
[a] Excluding patients with esophageal subepithelial tumors.

LSR (OR 18.940, 95% CI 3.623–99.007) were statistically significant independent predictors of a GIST diagnosis.

GISTs are known to arise predominantly in the stomach and intestines but are rarely documented in the esophagus [18]. Thus, a subgroup analysis was performed after excluding patients with esophageal SETs. In the multivariate logistic regression analysis of this subgroup, vascularity (OR 15.184, 95% CI 2.809–82.062) and the LSR (OR 14.280, 95% CI 2.593–78.637) were also identified as independent predictors of GIST.

3.3. Diagnostic value of non-invasive predictors

Using the validated parameters, we analyzed the diagnostic values for the noninvasive diagnosis of GIST, including sensitivity, specificity, PPV, NPV, and diagnostic accuracy. When noninvasive diagnosis of GIST was performed with low LSR, the sensitivity, specificity, PPV, NPV, and accuracy were 83.8%, 75.8%, 79.5%, 80.6%, and 80.0%, respectively. In case of vascularity, the sensitivity, specificity, PPV, NPV, and accuracy were 81.1%, 84.8%, 85.8%, 80.0% and 82.9%, respectively.

3.4. Prediction model for non-invasive diagnosis of GIST

We established a noninvasive prediction model of GIST through the CART model, by allocating patients according to statistically significant variables (vascularity and LSR). In CART analysis, the Gini index was used to measure impurity. For the 70 total patients, the final CART model consisted of 3 terminal nodes that included 2 variables: the LSR and vascularity. By using this model, patients who showed positive vascularity in the arterial phase were allocated to terminal node 1. If the patients showed negative vascularity, selection proceeded to the next step by using the LSR. If a patient's LSR was ≤1.475, the patient was allocated to terminal node 2, and patients with high LSR (>1.475) were allocated to terminal node 3. The sensitivity, specificity, and AUROC values of this noninvasive prediction model were 1 (1–1), 0.667 (0.506–0.828), and 0.893, respectively (Fig. 4A).

A total of 35 patients were allocated to terminal node 1. Among them, 85.7% (n = 30) were diagnosed as having GIST and only 5 patients had leiomyoma. Thirteen patients were allocated to terminal node 2, and 7 patients (53.8%) were diagnosed as having GIST. In terminal node 3, 22 patients were allocated, and all of these patients were diagnosed as having leiomyoma (100%).

If this algorithm is used in clinical practice, allocation to terminal node 1 may be defined as "suggestive of GIST," and physicians can recommend early endoscopic or surgical resection or close monitoring if the size of the SET is small. Likewise, allocation to terminal node 3 may be determined to indicate "suggestive of leiomyoma," and physicians can consider regular endoscopic follow-up only. For patients allocated to terminal node 2, the diagnosis may be somewhat complicated—pathological confirmation via biopsy is recommended unless the size is small. Because only about half of

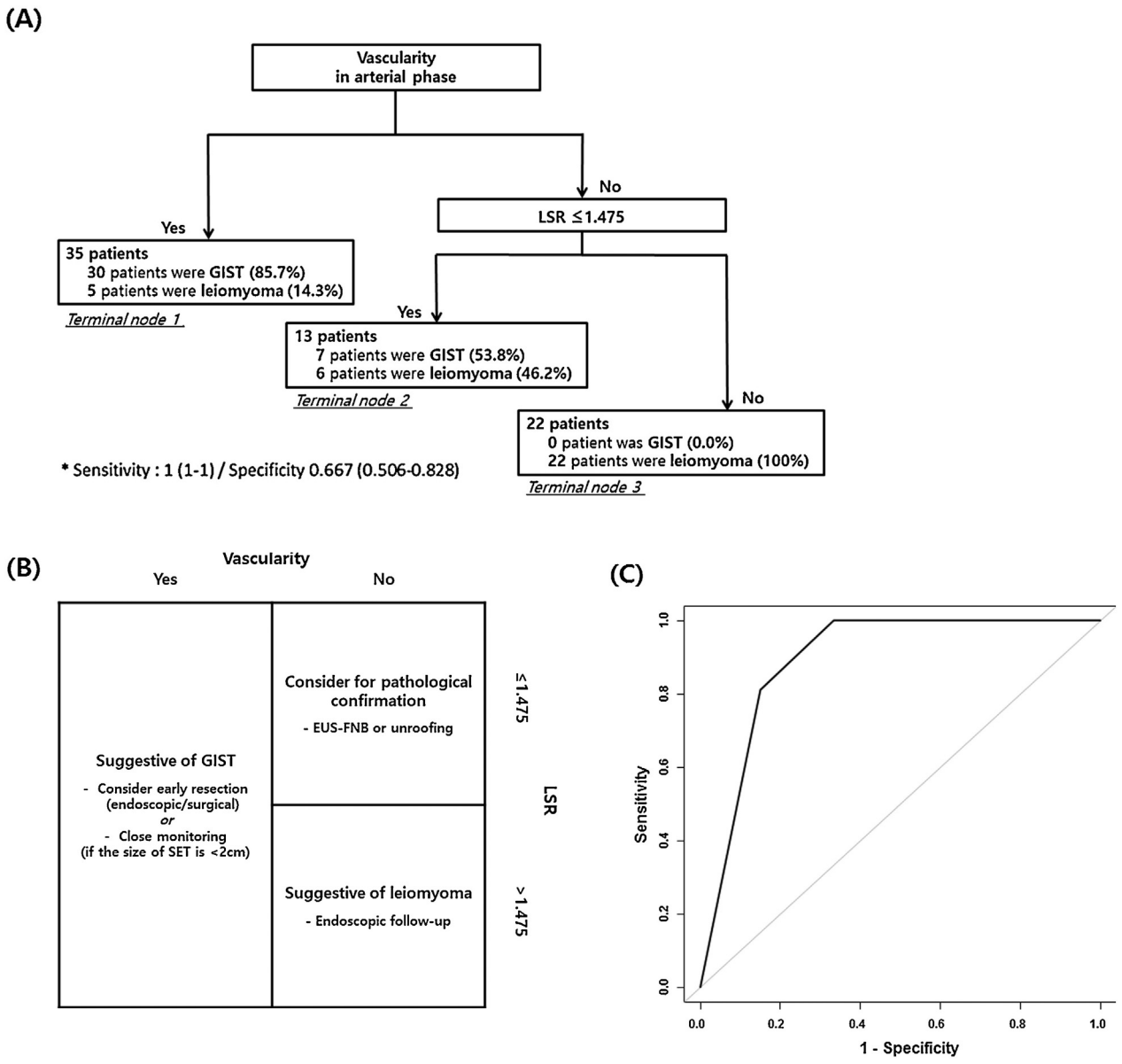

Fig. 4. Noninvasive prediction model for gastrointestinal stromal tumor (GIST) diagnosis using contrast-enhanced harmonic endoscopic ultrasound. Tree representation (A) and recursive partition (B) were generated using the classification and regression tree (CART) model. (C) Receiver-operating characteristic curve for the CART model (area under the curve, 0.893).

the patients were diagnosed as having GIST in this group, terminal node 2 can be determined to indicate "consider for pathological confirmation" (Fig. 4B). Moreover, the AUROC was 0.893 for the CART model (Fig. 4C).

4. Discussion

EUS is the most valuable diagnostic tool for evaluating the size, margin, layer of origin, and echogenicity of SETs [19]. However, although many studies have been performed for the noninvasive diagnosis of SETs through conventional EUS, the diagnostic accuracy was relatively low in the differential diagnosis of such tumors, especially those originating from the muscularis propria layer [3,4,20]. Some researchers suggested that the malignancy risk of SETs can be evaluated with conventional EUS by using specific findings such as tumor size, irregular border, internal heterogeneity, hyperechogenic foci, or cystic space [19,21,22]; however, the EUS findings mentioned above are not commonly found in small- to medium-sized SETs. Therefore, the differential diagnosis and malignancy risk stratification using EUS features are limited.

Recently, CEH-EUS was introduced to improve the diagnostic accuracy of conventional EUS without invasive biopsy procedures. By using second-generation contrast agents such as SonoVue (Bracco Imaging, Milan, Italy) and a harmonic imaging technique that suppresses background tissue signals, CEH-EUS can improve the detectability of small-vessel blood flow under echoendoscope transducers [23,24]. Several studies have claimed that CEH-EUS findings can be used as parameters for differentiating the malignant potential of GISTs. Recently published studies also used the intensity of enhancement and/or the pattern of CEH-EUS to discriminate between benign SETs and GIST. These studies showed high sensitivity (84.5%–100%), specificity (63%–100%), and accuracy (82.2%–83%) [14,15,25,26]. However, there are still limitations to the clinical application of using contrast pattern alone. In clinical practice, CEH-EUS findings alone are not sufficient to completely

evaluate the malignant potential of GISTs and to differentiate these tumors from other benign SETs.

Therefore, in this study, we attempted to establish a noninvasive prediction model of GISTs using CEH-EUS and other clinical factors. To differentiate from previous studies and establish a highly predictive model, we analyzed the contrast enhancement patterns by dividing them into 2 phases according to the timing of enhancement. Especially, we added the LSR as an easily measurable parameter in conventional B-mode. As a result, we obtained promising results with our prediction model. Among the 26 patients who had low LSR in B-mode and showed positive vascularity in CEH-EUS, 24 (92.3%) were diagnosed as having GIST, whereas all 22 patients (100%) who did not show vascularity and had high LSR were diagnosed as having leiomyoma.

The current National Comprehensive Cancer Network guidelines recommend that large (>2 cm) or small GISTs showing high-risk features on EUS (i.e., presence of echogenic foci or cystic space) should be resected. However, according to previous reports, up to 3.7% of GISTs <2 cm in size and without high-risk features on EUS have a high mitotic index and rapidly increase in size, and hence have a high malignant potential [27,28]. In this context, the European Society for Medical Oncology guideline recommends excision as the standard treatment for histologically proven small GISTs [29]. Therefore, if a GIST is suspected early through a noninvasive method, patients can be treated using a minimally invasive technique such as endoscopic resection, thus avoiding unnecessary operations, or they can be followed up more carefully.

In our study population, 27 (38.6%) patients presented with SET lesions <2 cm. To confirm the usefulness of the parameters and the established prediction model to discriminate between small lesions, we divided the patients into two groups, according to the lesion size (<2 cm and ≥2 cm) and performed a subgroup analysis. Our results showed that vascularity and the LSR were significant independent predictors of a GIST diagnosis in the small SET group (<2 cm); we also confirmed that the prediction model has good predictive power in small SETs (Supplemental Tables 1 and 2). Thus, the parameters used in our study and the established noninvasive prediction model may be useful for discriminating relatively small- to moderate-sized GISTs from leiomyomas.

Since the 1990s, the LSR has been known to have diagnostic value in the differential diagnosis of lymphadenopathy using radiological methods [30]. Steinkamp et al. reported that the LSR showed high accuracy (95%) in the differential diagnosis of cervical nodes [31]. Dragoni et al. showed that the LSR was significantly lower in neoplastic lymph nodes than in reactive lymph nodes [32]. The low LSR of malignant lymph nodes is associated with a growth pattern showing alteration of the hylus and cortex. As malignant lymph nodes tend to be round, the LSR is lower in these nodes than in reactive lymph nodes with an oval growth pattern. Likewise, we assumed that the growth patterns of GISTs and leiomyomas, which have different cell origins and malignant potential are also different. In this study, the GIST group had a significantly lower LSR than the leiomyoma group, and a high AUROC (0.856) was obtained when the cutoff value was determined through the receiver-operating characteristic curve. Although the utility of the LSR in differential diagnosis is not very popular, because of technological developments and emerging new parameters, the LSR can be used as a supplementary parameter to CEH-EUS findings, to intuitively increase the accuracy of the noninvasive diagnosis.

Most esophageal SETs with a mesenchymal origin are leiomyomas, whereas GISTs are uncommon in the esophagus. In this study, 15 of 33 leiomyomas were found in the esophagus; however, there was no GIST in the esophagus. To remove the confounding factor of the SET location, a subgroup analysis was done after excluding patients with esophageal SETs. Even after excluding patients with esophageal SETs, patients with GISTs still had a significantly lower LSR than those with leiomyomas (1.30 vs. 1.74, $p < 0.001$) (data not shown). The proportion of patients with positive vascularity was also significantly higher in the GIST group (81.1% vs. 27.8%, $p < 0.001$) (data not shown). Additionally, the LSR and vascularity were found to be useful as independent predictors of the noninvasive diagnosis of GIST in multivariate analysis.

We used the CART analysis in this study to establish the prediction model. The CART method was introduced by Breiman et al. in 1984 [33]. It enables the construction of a tree algorithm and recursive partitioning, allowing researchers to create a prediction model that can be intuitively interpreted. In this study, we established an efficient prediction model using a continuous variable (LSR) and a categorical variable (vascularity). However, owing to the instability due to overfitting, which is a disadvantage of CART, there is a limitation in its general application to other datasets. Therefore, for a more generalized prediction model, further studies in a larger population are needed. We hope that our research can be a starting point.

This study has several limitations. First, this is a single-center retrospective study with a relatively small number of cases. Only patients with pathologically confirmed disease were included, and data from patients without pathological confirmation owing to small tumor size or follow-up loss were excluded. Second, the qualitative CEH-EUS interpretation was made by only one endosonographer, which limits the measurement of interobserver variability. However, as the interpretation was only about the presence, not the degree, of vascularity, there will be no large ambiguity in the interpretation. Third, the optimal LSR cutoff value could not be firmly established in this study. Further large-scale prospective studies using additional imaging modalities are required for a more precise prediction. Despite these limitations, this study has a certain value as the first study to show the possibility of noninvasive diagnosis of GISTs, with a relatively high accuracy, by using CEH-EUS findings and the LSR.

In conclusion, the LSR and vascularity in CEH-EUS can be used as parameters for the noninvasive prediction model of GISTs. This noninvasive diagnostic model may be helpful in the early diagnosis, decision making, and treatment planning in patients with SETs.

Conflict of interest

None declared.

Appendix A. Supplementary data

Supplementary data associated with this article can be found, in the online version, at https://doi.org/10.1016/j.dld.2019.02.017.

References

[1] Hedenbro JL, Ekelund M, Wetterberg P. Endoscopic diagnosis of submucosal gastric lesions. The results after routine endoscopy. Surg Endosc 1991;5:20–3.
[2] Lim YJ, Son HJ, Lee JS, Byun YH, Suh HJ, Rhee PL, et al. Clinical course of subepithelial lesions detected on upper gastrointestinal endoscopy. World J Gastroenterol 2010;16:439–44.
[3] Humphris JL, Jones DB. Subepithelial mass lesions in the upper gastrointestinal tract. J Gastroenterol Hepatol 2008;23:556–66.
[4] Hwang JH, Saunders MD, Rulyak SJ, Shaw S, Nietsch H, Kimmey MB. A prospective study comparing endoscopy and EUS in the evaluation of GI subepithelial masses. Gastrointest Endosc 2005;62:202–8.
[5] Menon L, Buscaglia JM. Endoscopic approach to subepithelial lesions. Therap Adv Gastroenterol 2014;7:123–30.
[6] Miettinen M, Sobin LH, Lasota J. Gastrointestinal stromal tumors of the stomach: a clinicopathologic, immunohistochemical, and molecular genetic study of 1765 cases with long-term follow-up. Am J Surg Pathol 2005;29:52–68.
[7] Agaimy A. Gastrointestinal stromal tumors (GIST) from risk stratification systems to the new TNM proposal: more questions than answers? A review emphasizing the need for a standardized GIST reporting. Int J Clin Exp Pathol 2010;3:461–71.

[8] Hoda KM, Rodriguez SA, Faigel DO. EUS-guided sampling of suspected GI stromal tumors. Gastrointest Endosc 2009;69:1218–23.
[9] Wani S, Muthusamy VR, Komanduri S. EUS-guided tissue acquisition: an evidence-based approach (with videos). Gastrointest Endosc 2014;80, 939-59 e7.
[10] Iglesias-Garcia J, Poley JW, Larghi A, Giovannini M, Petrone MC, Abdulkader I, et al. Feasibility and yield of a new EUS histology needle: results from a multicenter, pooled, cohort study. Gastrointest Endosc 2011;73:1189–96.
[11] Kataoka M, Kawai T, Yagi K, Sugimoto H, Yamamoto K, Hayama Y, et al. Mucosal cutting biopsy technique for histological diagnosis of suspected gastrointestinal stromal tumors of the stomach. Dig Endosc 2013;25:274–80.
[12] Komanduri S, Keefer L, Jakate S. Diagnostic yield of a novel jumbo biopsy "unroofing" technique for tissue acquisition of gastric submucosal masses. Endoscopy 2011;43:849–55.
[13] Kim GH, Cho YK, Kim EY, Kim HK, Cho JW, Lee TH, et al. Comparison of 22-gauge aspiration needle with 22-gauge biopsy needle in endoscopic ultrasonography-guided subepithelial tumor sampling. Scand J Gastroenterol 2014;49:347–54.
[14] Park HY, Jeon SW, Lee HS, Cho CM, Bae HI, Seo AN, et al. Can contrast-enhanced harmonic endosonography predict malignancy risk in gastrointestinal subepithelial tumors? Endosc Ultrasound 2016;5:384–9.
[15] Sakamoto H, Kitano M, Matsui S, Kamata K, Komaki T, Imai H, et al. Estimation of malignant potential of GI stromal tumors by contrast-enhanced harmonic EUS (with videos). Gastrointest Endosc 2011;73:227–37.
[16] Piscaglia F, Nolsoe C, Dietrich CF, Cosgrove DO, Gilja OH, Bachmann Nielsen M, et al. The EFSUMB Guidelines and Recommendations on the Clinical Practice of Contrast Enhanced Ultrasound (CEUS): update 2011 on non-hepatic applications. Ultraschall Med 2012;33:33–59.
[17] Saftoiu A, Dietrich CF, Vilmann P. Contrast-enhanced harmonic endoscopic ultrasound. Endoscopy 2012;44:612–7.
[18] Miettinen M, Sarlomo-Rikala M, Sobin LH, Lasota J. Esophageal stromal tumors: a clinicopathologic, immunohistochemical, and molecular genetic study of 17 cases and comparison with esophageal leiomyomas and leiomyosarcomas. Am J Surg Pathol 2000;24:211–22.
[19] ASGE Standards of Practice Committee, Gan SI, Rajan E, Adler DG, Baron TH, Anderson MA, et al. Role of EUS. Gastrointest Endosc 2007;66:425–34.
[20] Karaca C, Turner BG, Cizginer S, Forcione D, Brugge W. Accuracy of EUS in the evaluation of small gastric subepithelial lesions. Gastrointest Endosc 2010;71:722–7.
[21] Nishida T, Kawai N, Yamaguchi S, Nishida Y. Submucosal tumors: comprehensive guide for the diagnosis and therapy of gastrointestinal submucosal tumors. Dig Endosc 2013;25:479–89.
[22] Palazzo L, Landi B, Cellier C, Cuillerier E, Roseau G, Barbier JP. Endosonographic features predictive of benign and malignant gastrointestinal stromal cell tumours. Gut 2000;46:88–92.
[23] Alvarez-Sanchez MV, Napoleon B. Contrast-enhanced harmonic endoscopic ultrasound imaging: basic principles, present situation and future perspectives. World J Gastroenterol 2014;20:15549–63.
[24] Unnikrishnan S, Klibanov AL. Microbubbles as ultrasound contrast agents for molecular imaging: preparation and application. AJR Am J Roentgenol 2012;199:292–9.
[25] Kannengiesser K, Mahlke R, Petersen F, Peters A, Ross M, Kucharzik T, et al. Contrast-enhanced harmonic endoscopic ultrasound is able to discriminate benign submucosal lesions from gastrointestinal stromal tumors. Scand J Gastroenterol 2012;47:1515–20.
[26] Kamata K, Takenaka M, Kitano M, Omoto S, Miyata T, Minaga K, et al. Contrast-enhanced harmonic endoscopic ultrasonography for differential diagnosis of submucosal tumors of the upper gastrointestinal tract. J Gastroenterol Hepatol 2017;32:1686–92.
[27] Jeong IH, Kim JH, Lee SR, Kim JH, Hwang JC, Shin SJ, et al. Minimally invasive treatment of gastric gastrointestinal stromal tumors: laparoscopic and endoscopic approach. Surg Laparosc Endosc Percutan Tech 2012;22:244–50.
[28] Kim MY, Jung HY, Choi KD, Song HJ, Lee JH, Kim DH, et al. Natural history of asymptomatic small gastric subepithelial tumors. J Clin Gastroenterol 2011;45:330–6.
[29] Casali PG, Abecassis N, Bauer S, Biagini R, Bielack S, Bonvalot S, et al. Gastrointestinal stromal tumours: ESMO-EURACAN Clinical Practice Guidelines for diagnosis, treatment and follow-up. Ann Oncol 2018;29(Supplement_4):iv68–78.
[30] Vassallo P, Wernecke K, Roos N, Peters PE. Differentiation of benign from malignant superficial lymphadenopathy: the role of high-resolution US. Radiology 1992;183:215–20.
[31] Steinkamp HJ, Cornehl M, Hosten N, Pegios W, Vogl T, Felix R. Cervical lymphadenopathy: ratio of long- to short-axis diameter as a predictor of malignancy. Br J Radiol 1995;68:266–70.
[32] Dragoni F, Cartoni C, Pescarmona E, Chiarotti F, Puopolo M, Orsi E. The role of high resolution pulsed and color Doppler ultrasound in the differential diagnosis of benign and malignant lymphadenopathy: results of multivariate analysis. Cancer 1999;85:2485–90.
[33] Breiman L, Friedman JH, Olshen RA, Stone CJ. Classification and regression trees. Monterey, CA: Wadsworth & Brooks/Cole Advanced Books & Software; 1984.